Pergamon

Journal of Structural Geology, Vol. 17, No. 12, pp. 1789 to 1792, 1995

0191-8141/95 $9.50+0.00

0191-8141(95)00065-8

Estimation of the variation in apparent displacement along normal fault traces refracted by differential compaction

XIANG WANG*

Geotectonic Institute, Xian Geological College, Xian, Shaanxi 710054, P.R. China

(*Received* 17 *October* 1994; *accepted* 1 *June* 1995)

Abstract—Initially planar fault surfaces can be refracted by differential compaction, sudden changes in the displacement gradient taking place at the contact of different lithologies. As a result, the original displacement pattern, e.g. a cone-type in an idealized case, can be changed into a zigzag-type, especially when the initial dip angle of the fault and differential compaction are high. Compared with pre- and syn-faulting compaction, post-faulting compaction is more likely to change the initial displacement pattern along normal faults which were active near the sediment surface. Based upon the assumption that compaction is homogeneous vertical strain, the original fault geometry and displacement pattern can be estimated by means of decompaction and related geometric calculations.

INTRODUCTION

In idealized cases, displacement along fault traces varies from zero at the tip to a maximum value at the centre (Muraoka & Kamata 1983, Rippon 1985, Watterson 1986, Barnett *et al.* 1987). The displacement along such a fault trace will have a cone-shaped distribution pattern (C-type) on a diagram of trace length (L) vs displacement (D). However, C-type displacement is not the only displacement pattern identified along fault traces. Muraoka & Kamata (1983) reported an M-type displacement pattern that has a broad, central high-value portion, without significant changes of slope, and flanking portions with steep slopes. Peacock (1991) illustrated E- and D-type displacement distribution patterns on a normalized d–x diagram, where d is the displacement at the measurement point, and x is the distance between the maximum displacement point and the measuring point. The E- and D-types were defined as a displacement curve, elevated or depressed respectively, on the background of a C-type curve on a normalized d–x diagram. In order to interpret the existence of non-C-type displacement patterns, a number of possible controlling factors have been outlined. These include lithological difference, profile effect, influence of neighbouring faults (Muraoka & Kamata 1983) or linkages of fault segments (Ellis & Dunlap 1988), conjugate relationships, lithological variation and fault bends (Peacock 1991). Davison (1987) studied normal fault geometry related to burial and compaction. He claimed that passive vertical compaction of a fault plane can lead to a decrease in apparent fault displacement.

This paper is concerned with the influence of differential compaction on the displacement pattern along normal fault traces developed within multi-layered successions. The problem addressed also takes into account the relationship between the original geometry of faults and differential compaction. On the basis of some simplifying assumptions and using relevant geometric methods, an estimate of the variation of displacement distribution along a refracted normal fault trace is discussed.

DIFFERENTIAL COMPACTION AND DECOMPACTION OF FAULT PROFILES

Compaction in sedimentary rocks is caused by a progressive increase in overburden load and results in a corresponding reduction of porosity. In multi-layered successions, compaction is differential because various lithologies have a different response to the same overburden load. As a result of differential compaction within a multilayered succession, a pre-existing fault may change from a planar to a non-planar geometry (Fig. 1). The resultant displacement distribution pattern along the refracted fault trace can differ from that of the trace prior to compaction. To determine the original displacement distribution along a fault trace, the sedi-

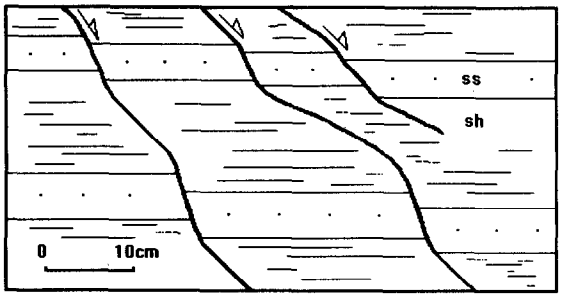

Fig. 1. Schematic section indicating the refraction of normal fault traces cutting through alternating Carboniferous sandstone and shale in the Tenby area, SW Wales; ss = sandstone, sh = shale.

*Present address: Department of Applied Geology, School of Mines, University of New South Wales, Sydney, NSW 2052, Australia.

mentary succession and the fault profile contained therein should be decompacted.

In this paper, compaction is taken as vertical shortening and only faults which were originally planar, normal and active near the sediment surface are considered. Growth faults are excluded because they usually display a maximum displacement at the top of the trace, as well as possibly involving listric detachment and differential strain within the hanging wall and foot wall across the fault (Waltham 1990). The assumption that compaction is homogeneous vertical shortening is inapplicable where strong horizontal strain is also obviously involved. However, such an approximation is acceptable under certain conditions, if it is supported by field observation (Davison 1987). Based on the above assumptions for compaction and faulting, the decompaction procedure discussed here mainly involves removal of the post-faulting compaction component. A pre- or syn-faulting compaction component may also exist, but its effect on the fault displacement pattern is probably very minor because compaction near the sediment surface is minimal.

Decompaction can be carried out by different methods involving porosity-depth function (Athey 1930, Sclater & Christie 1980, Gallagher 1989), solidity- or density-depth function (Hamilton 1976, Baldwin & Butler 1985) and the relative compaction between different lithologies (Davison 1987). Once the decompacted thickness of a layer (T) is known, the original dip (α) of the fault segment within an individual layer can be easily determined by the equation:

$$\alpha = \arctan\,(T/L_v), \qquad (1)$$

where L_v is the vertical projection length of the fault trace through an individual layer and T can be calculated through decompaction, assuming a porosity-depth function. By repeating this procedure for each segment of the refracted fault trace, the initial geometry of the fault can be reconstructed.

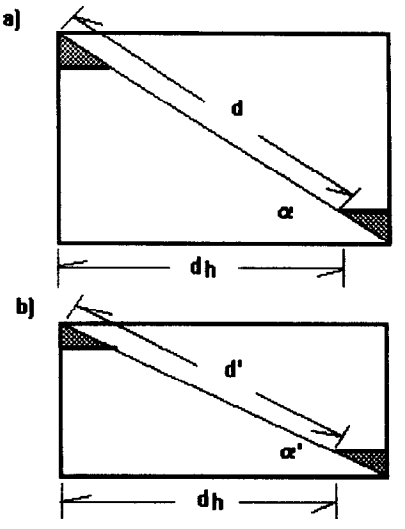

Fig. 2. (a) Normal fault with displacement, d, where d_h = heave, α = angle of dip. (b) Same fault after compaction (no horizontal strain), with displacement d_c where d_h = heave, α' = angle of dip.

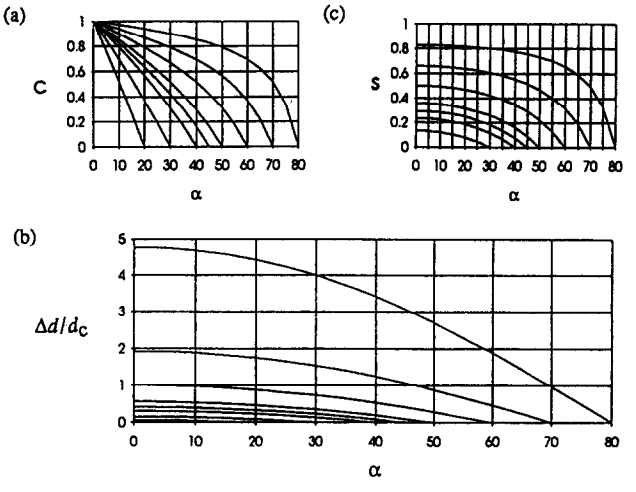

Fig. 3. Theoretical relationship between the decrease of the angle of dip of faults (α) and; (a) compaction (C); (b) reduction of displacement due to compaction; and (c) reduction of displacement.

ESTIMATION OF DISPLACEMENT ALONG DECOMPACTED FAULT TRACES

Variation in the displacement along a refracted fault trace depends upon the initial geometry of the fault and the compaction of adjacent sediments. If the original dip (α) of the fault segment is known, the displacement reduction (Δd) caused by compaction on a given fault segment can be obtained using

$$\Delta d = d - d_c = d_c = d_c(\cos\alpha'/\cos\alpha - 1) \qquad (2)$$

where d and d_c are the displacement along the fault segment before and after compaction (Fig. 2).

Figure 3(a) illustrates the relationship between compaction (C) and the variation of dip (α) of faults. With increased compaction, curves representing faults with a low initial dip descend at an almost steady rate, whilst curves for faults with a high initial dip descend at an increasing rate. Note that under the same compaction there is greater displacement drop for faults with a higher initial dip than those with low initial dip. For example, under a compaction of 30%, the resultant drop in displacement on three faults with an initial dip of 70°, 60° and 45° is $0.35d_c$, $0.27d_c$ and $0.159d_c$, respectively (Fig. 3b). The corresponding shortening of the displacement because of compaction is 25.9%, 19.7% and 13.7%, respectively (Fig. 3c). These, therefore, indicate that greater shortening or variation of displacement is likely on faults with high initial angle of dip.

In the case of a large fault cutting through a crystalline basement–sedimentary cover contact, differential compaction can have a distinct effect on the cover rocks, but little on the competent basement rocks. A discontinuity in the displacement gradient therefore tends to occur at the contact. As a result, the angle of dip on this fault may

gradually decrease with depth, but will suddenly become steeper (approximating the initial angle of dip) at the contact.

DISCUSSION

Because the effects of differential compaction cause refraction of the fault plane, the individual segments of that fault have different variation in displacement. This also produces a change in the initial displacement gradient along the fault trace. An interesting question is to what degree and under what conditions differential compaction can exert a significant influence on the displacement distribution pattern in vertical sections. Can it change the original displacement pattern?

Figure 4(a) (right) is taken from an imaginary case in which a planar fault dipping at 70° cuts through alternating sandstone and shale. The initial displacement distribution of this fault is taken as C-type (Fig. 4a, left). Two theoretical cases can now be considered. In the first case, the post-faulting compaction for sandstone and shale is taken as 10% and 30%, respectively. As a result, the dip of the fault is lowered to 68° in sandstones and 63° in shales (Fig. 4b, right). The resulting variation of displacement as a result of compaction is $0.1d_c$ for segments in sandstones and $0.4d_c$ in shales. Although there are local changes in displacement gradient, the displacement distribution pattern as a whole still remains C-type (Fig. 4b, left). In the second case, the compaction for sandstone and shale is taken as 20% and 60%, respectively, leading to a decrease in the angle of dip being lowered to 66° in sandstones and 48° in shales (Fig. 4c, right). The corresponding reduction in displacement is $0.2d_c$ for segments in sandstones and up to $0.9d_c$ in shales. The resulting displacement distribution is no longer C-type, but belongs to a zigzag type. Ellis and Dunlap (1988) described a zigzag displacement pattern produced by the linkage of individual fault segments with minimal displacement at the linkage points, which is obviously different in origin from that proposed here. In response to variation in the initial C-type displacement in beds of sandstone and shale caused by differential compaction, a fault with an initial planar geometry can be transferred into one with a zigzag displacement pattern.

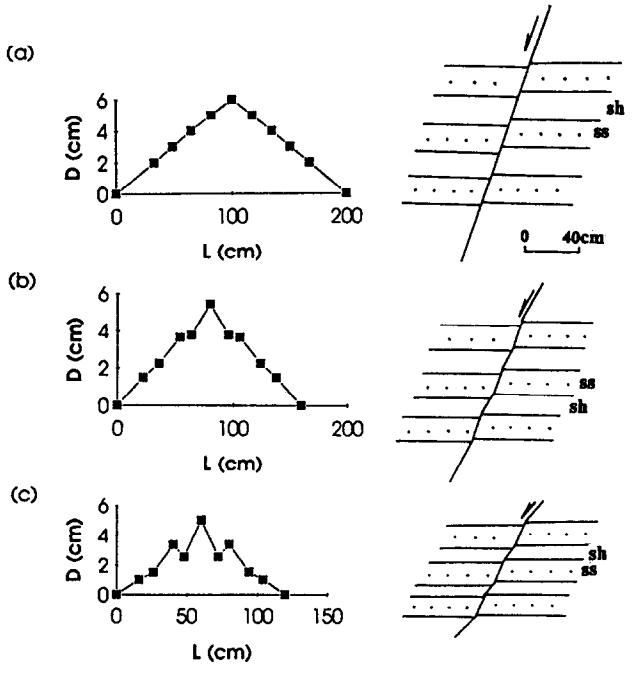

Fig. 4. (a) An assumed normal fault dipping at 70° cutting through alternating sandstone (ss) and shale (sh) (right) and corresponding displacement distribution pattern of this fault (left), which is cone-type (C-type). D = displacement, L = length of fault trace. (b) The same fault after differential compaction of 10% for sandstone and 30% for shale (right) and the corresponding displacement pattern (C-type) (left). (c) The same fault after differential compaction of 20% for sandstone and 60% for shale (right). At left: resultant displacement pattern that developed to a zigzag-type.

In examples given here, displacement and compaction are treated as separate processes in order that the component of displacement caused by compaction can clearly be distinguished from that of the initial displacement on the fault. However, fault displacement can take place as a compaction–strain–accommodation process, which means that syn-faulting and pre-faulting compaction may be involved, besides post-faulting compaction. In the case of extensive compaction before faulting, the initial fault geometry may become non-planar and the consequent displacement along such a refracted fault trace may produce pull-apart structures along the segments with higher angles of dip. Since this paper focuses on faults that are active near the sediment surface where compaction is minimal, pre-faulting compaction is likely to have a minor effect on the pattern of fault displacement. Syn-faulting compaction, which can lead to a build-up of shear stress along faults, is unlikely to change the final overall pattern of displacement on an active fault because new fractures in this case will tend to develop at the tips of the fault (Cowie & Scholz 1992), the maximum displacement being generally proportional to the fault dimension (Watterson 1986). On the other hand, compaction near the sediment surface is always weak.

CONCLUSION

The geometry of normal faults that are active close to the surface of a sedimentary succession may be affected by post-faulting compaction. The refraction of fault traces can be caused by an abrupt change in displacement gradient at the contact of different lithological units. This may significantly change the initial pattern of displacement, especially where both the initial dip angle of the fault and differential compaction are high. In this case, differential compaction is likely to lead to the development of a zigzag-type displacement pattern.

Assuming that compaction is homogeneous vertical strain, the variation in displacement caused by compaction can be estimated and the initial pattern of displacement can be reconstructed by decompaction and simple geometric calculations.

Acknowledgements—The author is grateful to John Roberts for correcting the English of an early version of this manuscript. This paper benefited greatly from the critical comments of Ian Davison and another anonymous referee.

REFERENCES

Athy, L. F. 1930. Density, porosity and compaction of sedimentary rocks. *Bull. Am. Ass. Petrol. Geol.* **14**, 1–24.

Baldwin, B. & Butler, C. O. 1985. Compaction curves. *Bull. Am. Ass. Petrol. Geol.* **69**, 622–626.

Barnett, J. A. M., Mortimer, J., Rippon, J. H., Walsh, J. J. & Watterson, J. 1987. Displacement geometry in the volume containing a single normal fault. *Bull. Am. Ass. Petrol. Geol.* **71**, 925–937.

Cowie, P. A. & Scholz, C. H. 1992. Physical explanation for the displacement–length relationship of faults using a post-yield fracture mechanics model. *J. Struct. Geol.* **10**, 1133–1148.

Davison, 1987. Normal fault geometry related to sedimentary compaction and burial. *J. Struct. Geol.* **9**, 393–402.

Ellis, M. A. & Dunlap, W. J. 1988. Displacement variation along thrust faults: implication for the development of large faults. *J. Struct. Geol.* **10**, 183–192.

Gallagher, K. 1989. An examination of some uncertainties associated with estimate of sedimentation rates and tectonic subsidence. *Basin Res.* **2**, 97–114.

Hamilton, E. L. 1976. Variation of density and porosity with depth in deep sea sediments. *J. sedim. Petrol.* **46**, 280–300.

Muraoka, H. & Kamata, H. 1983. Displacement distribution along minor fault traces. *J. Struct. Geol.* **5**, 483–495.

Peacock, D. C. P. 1991. Displacements and segment linkage in strike-slip fault zones. *J. Struct. Geol.* **13**, 1025–1035.

Reike, H. R. & Chilingarian, G. V. (eds) 1974. *Compaction of Argillaceous Sediments. Developments in Sedimentology*, p. 16. Elsevier, Amsterdam.

Rippon, J. 1985. Contoured patterns of the throw and hade of normal faults in the coal measures (Westphalian) of north-east Derbyshire. *Proc. Yorks. geol. Soc.* **45**, 147–161.

Sclater, J. G. & Christie, P. A. F. 1980. Continental stretching: an explanation of the post-mid-Cretaceous subsidence of central North Sea basin. *J. geophys. Res.* **85**, 3711–3739.

Shelton, J. W. 1962. Shale compaction in a section of Cretaceous Dakota sandstone, northwestern Dakota. *J. sedim. Petrol.* **32**, 873–877.

Waltham, D. 1990. Finite difference modeling of sandbox analogue, compaction and detachment-free deformation. *J. Struct. Geol.* **12**, 375–381.

Watterson, J. 1986. Fault dimensions, displacements and growth. *Pure & Appl. Geophys.* **124**, 365–373.